Residual Opening of Hydraulic Fractures Filled with Compressible Particles

Luiz Bortolan Neto, Andrei Kotousov

School of Mechanical Engineering, The University of Adelaide, Adelaide SA 5005 Australia

luiz.bortolanneto@adelaide.edu.au, andrei.kotousov@adelaide.edu.au

Abstract

Hydraulic stimulation technologies are currently widely applied across resource and power generation industries to increase productivity of oil/gas or hot water reservoirs. These technologies utilise a pressurised fluid, which is applied inside the well to initiate and drive fractures as well as to open a network of natural fractures. To prevent the opened fractures from complete closure during production stage, small particles (proppants) are normally injected with the pressurised fluid. These particles are subjected to confining stresses when the fluid pressure is removed, which lead to a partial closure of the opened fractures. The residual fracture openings are the main outcome of such hydraulic stimulations as these openings significantly affect the permeability of the reservoirs and, subsequently, well productivity. Past research was largely focused on the assessment of conditions and characteristics of fluid driven fractures as well as proppant placement techniques. Surprisingly, not much work was devoted to the assessment of the residual fracture profiles. In this work we develop a simplified non-linear model of residual closure of a crack filled with deformable particles under remote compressive stresses. It is demonstrated that the closure profile is significantly influenced by the distribution and compressibility of the particles, which are often ignored in the existing analytical or semi-analytical models.

Keywords: Hydraulic well stimulation, Well productivity, Fluid driven fractures, Proppant, Fracture residual opening, Residual crack closure, Distributed Dislocation technique.

1. Introduction

The problem under consideration has many important applications in gas/oil recovery technologies associated with hydraulic stimulation of underground reservoirs (Kotousov et al. 2011). These technologies can provide a significant enhancement of the permeability of geological reservoirs and often result in a considerable increase in the well productivity (Economides and Nolte 2000). The well stimulation procedures typically incorporate an injection of small particles (proppant) in order to keep the artificial fractures or network of natural cracks (faults) open throughout the production stage. During this stage the hydraulic pressure is removed in order to facilitate oil or gas recovery (Golf-Racht 1982; Barenblatt et al. 1990) and the in situ stresses lead to a partial closure of the fracture channels (Walsh 1981; Pyrak-Nolte et al. 1987). As the permeability of the fractured reservoir is strongly affected by the apertures of the fractures, the determination of the residual opening and fracture channel permeability filled with injected particles is of great practical interest (Vincent 2002).

Over the past fifty years many sophisticated solutions have been developed to evaluate the fluid-driven fracture geometries during hydraulic stimulations (Adachi et al. 2007). In the same time, a number of effective techniques were developed to simulate various proppant transport phenomena and the proppant placement along such fractures. These solutions and techniques are currently widely utilised in industry and were comprehensively discussed in many review papers and books by many researchers, such as Warpinski et al. (1994), Mahrer (1999), Economides and Nolte (2000), and Rahman and Rahman (2010) to name a few. Nevertheless, the evaluation of the residual fracture profiles, which are directly linked to fracture conductivity as mentioned above, has received much less attention. For example, Papanastasiou (2000) and Dam et al. (2000) utilised oversimplified models to assess the residual fracture profiles but merely neglected the proppant compressibility and its distribution inside the fracture. A recent study by Kotousov (2011) deals with the final opening of two semi-infinite planes compressing a rigid circular inclusion of elastic-linear behaviour. Kotousov's work is of great practical interest in situations where the hydraulic fracture length is not known a priori and it is supported by individual particles. Nevertheless, this

is not an ideal solution to simulate the residual opening of a hydraulic fracture supported by a pack of proppant with non-linear behaviour.

The evaluation of the well productivity is typically based on elliptical or constant thickness shapes of fracture openings (e.g. Zazovskii and Todua 1991; Entov and Murzenko 1994; Murzenko 1994; Kanevskaya and Kats 1996), which cannot be considered as realistic fracture shapes for many practical applications. In addition, the well productivity estimates often relay on the assumption that the fracture is fully filled with proppant and make radical simplifications regarding incompressibility of the proppants. One of the objectives of this paper is to evaluate the validity of some of these assumptions and simplifications.

The propping agents utilised in hydraulic fracturing are simply an assembly (pack) of unconsolidated granular particles (sand is often used as the proppant agent), which was the subject of many research papers in the past (Panayiotopoulos 1989). Initially, the pack of particles is highly compressible due to an initially small contact area between the particles and pack rearrangement under loading. Therefore, it is expected that the initial compressibility of the proppant inside the fracture has a considerable effect on the residual fracture opening and, consequently, on the fracture conductivity (Cutler et al. 1985; Montgomery and Steanson 1985). The residual fracture opening is also significantly affected by the transport and distribution of proppants within the fracture (Cutler et al. 1985; Montgomery and Steanson 1985). This will be discussed next.

In a pioneering study, Kern et al. (1959) reported their findings related to transport and settling of proppant (sand) near the wellbore in vertical hydraulic fractures. In this study it was presented experimental evidences of the development of a mound of settled sand on the bottom face of a vertical fracture, as illustrated in Fig. 1. It was also demonstrated that the proppant build up develops and grows until the injected fluid flow velocity is high enough and greater than some critical velocity.

After the initial study of Kern et al. (1959), a few other experimental works on proppant transport and settling were conducted, for example, the work by Wahl and Campbell (1963). These experimental studies were also supported by mathematical and numerical modelling. Daneshy (1975; 1978) was one of the first researchers who proposed a simplified model for the proppant transport and settling in hydraulic fractures. This model was further extended by Novotny (1977). In these theoretical developments it was assumed that the proppant transport and settling follows Stokes' law. Novotny's model, however, also incorporates a highly simplified model for an estimate of the residual opening of a hydraulic fracture. These works and many others were thoroughly reviewed by Clark and Güler (1983). After these early studies, more advanced and complex models for the transport and settling of proppants have been proposed, as, for instance, the ones by Clifton and Wang (1988), Unwin and Hammond (1995), Smith and Klein (1995), and, more recently, Gadde et al. (2004).

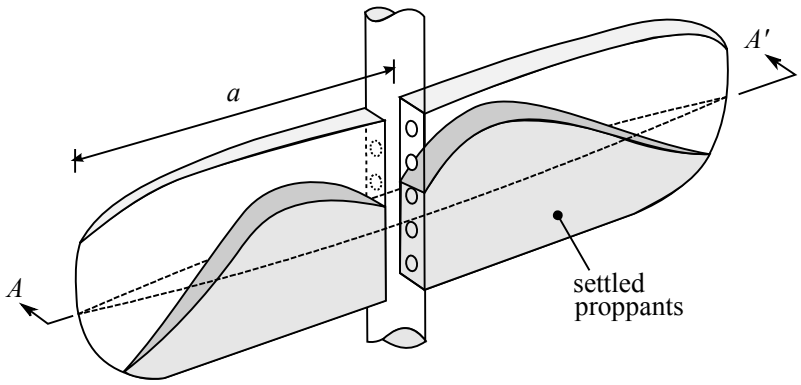

Fig. 1 Proppant build up in a hydraulic fracture. The cross section AA' is depicted in detail in Fig. 2a (not to scale)

From what was discussed above it becomes clear the hydraulic fracturing of rock formations is a very complex three-dimensional (3D) problem that involves the occurrence of several physical phenomena. A comprehensive comparative study between two- and three-dimensional simulators was provided by Warpinski et al. (1994) whereas a brief review on more recent 3D models was presented by Secchi and Schrefler (2012). Although 3D models allow a more comprehensive analysis of the fracture propagation and fracture geometry, a significant amount of data is required to justify their use and considerable computation effort is demanded.

Moreover, even 3D models require the adoption of an idealised geometry in order to derive effective and useful solutions (Adachi et al. 2007).

In the current study we made an effort to develop a simple nonlinear mathematical model capable of predicting the residual opening of a hydraulic fracture taking into account both the proppant distribution and its compressibility. The developed model can also be useful to understand, investigate and describe the stress state around the fracture due to the residual opening. The solution approach is based on the Distribution Dislocation Technique (DDT) and the Gauss-Chebyshev quadrature. It provides an effective way to solve many complicated Fracture Mechanics problems. One example is considered in the Appendix.

A detailed description of the mechanical model and its underpinning theory will be presented in the next Section. This model is followed by a mathematical formulation and the solution approach. A discussion of obtained results and conclusions regarding the main outcomes of the current work will be provided in the final section of this paper. In the Appendix a verification study is conducted and results are compared with an analytical solution of a problem having a very similar mathematical formulation but belonging to a completely different area.

2. Mechanical Model and Boundary Conditions

The shape and structure of hydraulically driven fractures are normally very complex (Rahman and Rahman 2010). Any approach (analytical or numerical) to the description and evaluation of the hydraulically driven fractures will require some radical simplifications. It is important to highlight that currently it is practically impossible to avoid many of these simplifications. In the mechanical model to be developed in the current paper we just eliminate some of the most essential and critical simplifications associated with the distribution of the proppant along fracture and its incompressibility. Therefore, the considered model can be considered as a step improvement to the existing models widely utilised in gas and petroleum industries. It is expected that this model will be more adequate in the description of realistic fracture profiles and will allow evaluating the effect of various parameters, which are related to the hydraulic stimulation techniques, on the well productivity.

It is obvious that despite the presence of propping agents inside the fracture, the action of the confining stresses, σ^{∞}, will lead to a reduction $\Delta(x)$ in the fracture opening, as illustrated in Fig. 2. This reduction depends on the proppants mechanical response to the compressive loading as well as its distribution inside the fracture.

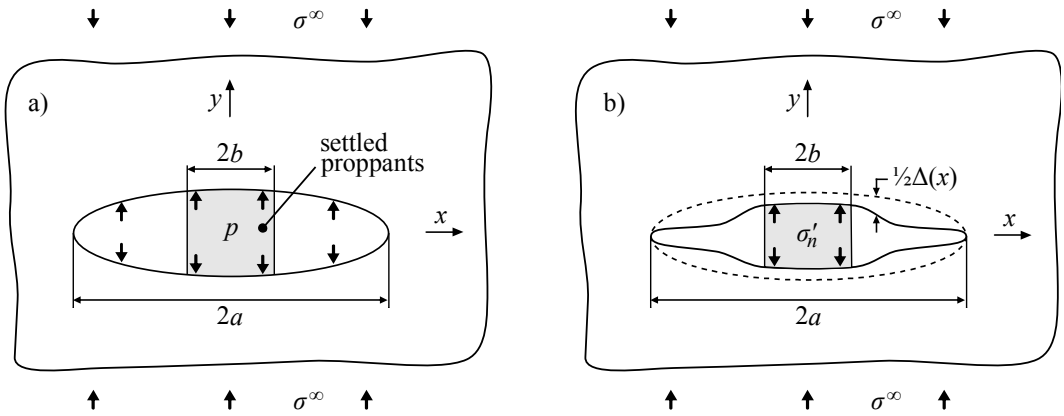

Fig. 2 The opening of a fracture due to an internal pressure p (a) is reduced after such pressure is removed (b). The hydraulic fracture full closure is prevented by the normal effective stress acting on the proppant, σ_n'

To find the residual fracture profile (Fig. 2b) we do have to introduce essential simplifications. The most radical simplification is that the fracture is considered to be a two-dimensional (2D) centred straight crack located along the line segment $|x| \leq a$, $y = 0$, subjected to plane strain conditions. This is a typical assumption utilised in almost all analytical studies conducted in the past which is valid only for elastic rock formations (Papanastasiou 2000). Further, the surrounding medium is assumed to be impermeable, isotropic, homogeneous, and linearly elastic with Young's modulus E and Poisson's ratio ν. The crack is subjected to a remote, normal, uniform compressive stress, $\sigma^{\infty} < 0$, such that

$$\sigma_{yy}(x^2 + y^2 \to \infty) = \sigma^{\infty}. \tag{1}$$

According to the Linear Elastic Fracture Mechanics, a constant fluid pressure, $p > 0$, inside the fracture will lead to an fracture initial opening $\delta_0(x)$, see Fig. 2a, given by the well-known expression:

$$\delta_0(x) = 4\frac{\sigma^\infty + p}{\bar{E}}\sqrt{a^2 - x^2}; \tag{2}$$

where σ^∞ has negative sign, $\bar{E}$ being the reduced Young's modulus defined as: $\bar{E} = E$, for plane stress, and $\bar{E} = E/(1-\nu^2)$, for plane strain. Additionally, the initial stress intensity factor due to the applied pressure can be written as

$$K_0 = (\sigma^\infty + p)\sqrt{\pi a}. \tag{3}$$

After the reduction, or total removal of the fluid pressure within the fracture during the stimulation stage, the proppants will be subjected to the remote compressive stress (or overburden pressure). It will prevent the full closure of the crack (as illustrated in Fig. 2b). The residual opening $\delta(x)$, being $\delta(x) = \Delta(x) + \delta_0(x)$, to be obtained from the problem governing equations, which will be discussed in the next section.

From the mechanical model described above it is possible to formulate the boundary-value problem that will define the residual shape of the fracture opening. The boundary conditions for the problem are as follows:

$$\sigma_{yy}(x,y) = \sigma^\infty, \qquad x^2 + y^2 \to \infty; \tag{4a}$$

and, at $y = 0$,

$$\sigma_{yy}(x,y) = \sigma_n', \qquad |x| \le b; \tag{4b}$$

$$\delta(x) = 0, \qquad |x| > a; \tag{4c}$$

where b is the settled proppants length (see Fig. 2) and σ_n' is the normal effective stress acting on the proppants. The latter depends both on the fracture residual opening and on the mechanical properties of the proppant. Next, the problem governing equations will be presented followed by a model for the mechanical response of a pack of proppant.

3. Governing Equations

From the boundary conditions introduced in the previous Section along with the help of the Distribution Dislocation Technique it is possible to set a system of the governing equations for the problem. These equations will be derived below for

arbitrary mechanical response of the proppant pack, which will be formulated in the next section.

In their classic work Bilby and Eshelby (1968) postulated that the perturbation of the uniform stress field in a body owing to the presence of a fracture may be deemed due to the existence of a distribution of dislocations along $|x| \leq a$, $y = 0$. Therefore, for the boundary conditions of the problem formulated above, the stresses along the fracture opening can be found from the corresponding Airy stress functions based on the unknown dislocation density $\rho(x)$ such that

$$\sigma_{xx}(x) = \frac{\overline{E}}{4\pi} \int_{-a}^{a} \frac{\rho(\xi)}{x - \xi} \mathrm{d}\xi \tag{5}$$

and

$$\sigma_{yy}(x) = \frac{\overline{E}}{4N} \int_{-a}^{a} \frac{\rho(\xi)}{x - \xi} \mathrm{d}\xi + \sigma^{\infty}. \tag{6}$$

The out-of-plane stress component being a consequence of the accepted plane strain assumption is then given by

$$\sigma_{zz}(x) = \nu \Big(\sigma_{xx}(x) + \sigma_{yy}(x) \Big). \tag{7}$$

The dislocation density is not known a priori and can be obtained from the solution of the problem. Therefore, the dislocation density $\rho(x)$ can be found from the following integral equation:

$$\frac{\overline{E}}{4\pi} \int_{-a}^{a} \frac{\rho(\xi)}{x - \xi} \mathrm{d}\xi = -\sigma^{\infty} + \sigma_n', |x| \leq a. \tag{8}$$

The requirement that the net content of the dislocations must be vanished at the fracture ends gives rise to the following additional single-value condition which also has to be satisfied (Kotousov and Codrington 2010):

$$\int_{-a}^{a} \rho(\xi) \mathrm{d}\xi = 0. \tag{9}$$

The fracture residual opening, (x), is then given by (Hills et al. 1996)

$$\delta(x) = -\int_{-a}^{x} \rho(\xi)\mathrm{d}\xi. \tag{10}$$

The exact solution of the integral equations (8) and (9) introduced above is not straightforward and requires an inversion of the left hand side integral in Eq. (8). Nonetheless, an effective solution may be obtained by the employment of numerical and computational methods, which will be discussed later in this paper.

4. Mechanical Behaviour of a Pack of Compressible Particles

One possible approach to evaluate the elastic properties of low consolidated media was recently presented by Bortolan Neto et al. (2011a; 2011b) and it will be employed here to complete the mathematical formulation of the problem. In this approach the particles are assumed to be of spherical shape, having a small contact area and the deformation of the particles follows the classical Hertz contact theory (Hertz 1896; Johnson 1982; Johnson 1985). Under such conditions the porosity of the medium is close to the percolation limit, which allows an application of simplified analytical techniques. It was demonstrated that the approach developed by Bortolan Neto et al. (2011a; 2011b) can adequately describe the combined behaviour of non-consolidated particles near the percolation limit and provides a good agreement with experimental results.

If E_s is the Young's modulus and ν_s is the Poisson's ratio of the particles, the relationship between the bulk modulus of elasticity of the pack of particles (either saturated or not) and the elastic properties of the single particle is given by (Bortolan Neto et al. 2011b):

$$\begin{aligned} B_m = \frac{\omega E_s}{1-\nu_s^2}\sqrt{\frac{\gamma\omega\varepsilon_{vm}}{2}} + B_f\frac{\phi}{\phi_0}\left(\frac{3}{2}\gamma\omega(1-\phi)\sqrt[3]{\frac{1-\phi}{1-\phi_0}} + \frac{\phi}{1-\varepsilon_{vm}}\right) \\ - B_f\frac{3}{2}\gamma\omega(1-\phi)\sqrt[3]{\frac{1-\phi}{1-\phi_0}}\ln\left(\frac{\phi}{\phi_0}(1-\varepsilon_{vm})\right). \end{aligned} \tag{11}$$

The relationship for the volumetric strain (dilatation), ε_{vm}, as a function of porosity, ϕ, being (Bortolan Neto et al. 2011b)

$$\varepsilon_{vm} = \frac{2}{\gamma\omega}\left(1 - \sqrt[3]{\frac{1-\phi_0}{1-\phi}}\right); \tag{12}$$

with B_f being the fluid bulk modulus, ϕ_0 the initial porosity of the particles assembly, γ the contact area parameter and ω the packing constant. The latter two variables can be represented as a function of ϕ_0 and are given, respectively, by (Bortolan Neto et al. 2011b)

$$\omega = 0.0207\phi_0^{-2.783} \tag{13}$$

and

$$\gamma = \exp(5\phi_0)/3. \tag{14}$$

Using the well known relationship between the longitudinal modulus and the bulk modulus,

$$M_m = 3B_m\frac{1-\nu_m}{1+\nu_m}, \tag{15}$$

and taking into account that for low consolidated particles $\nu_m \approx 0$, the following relationship can be obtained:

$$M_m = 3B_m. \tag{16}$$

The particle pack final porosity, ϕ, can be found iteratively from

$$\sigma_n' = M_m(\phi)\varepsilon_m(\phi), \tag{17}$$

where the uniaxial strain, ε_m, is found to be (Bortolan Neto et al. 2011b):

$$\varepsilon_m = 1 - \sqrt[3]{\frac{1-\phi_0}{1-\phi}}. \tag{18}$$

It is important to highlight that the presented is just one of several other models available in the literature and there is no conceptual limitation that prevents the utilisation of more complicated or more comprehensive theories in the current mathematical formulation.

5. Solution Procedure

The governing integral equation, Eq. (8), has singular behaviour at the ends of the integration interval and it has to be solved for the unknown density of dislocations, $\rho(x)$. As it was pointed out above, an exact solution is not straightforward since the inversion of the left hand side of the equation is required. Furthermore, the singularity of the Cauchy kernel of the integral, $(x-\xi)^{-1}$, prevents the utilisation of common numerical integration methods to obtain an accurate solution, specifically at the singular points. Nevertheless, there are a number of numerical procedures that can be effective in handling singular behaviour of the solution function. One of such procedures is the Gauss-Chebyshev quadrature method, which was employed in the current paper to generate the numerical results. It will be discussed next.

5.1 Numerical formulation

The first step in deriving a proper numerical solution method is to introduce normalising parameters over the interval $[-a, +a]$. Therefore,

$$s = \xi / a \tag{19a}$$

and

$$t = x/a. \tag{19b}$$

Thus, as the dislocation density $\rho(s)$ tends to infinity in a square root singular manner as $|s|$ approaches the unity, the dislocation density can be expressed as a product of the fundamental solution, $1/\sqrt{1-s^2}$, and an unknown regular function, $\psi(s)$, such that (Hills et al. 1996):

$$\rho(s) = \frac{\psi(s)}{\sqrt{1-s^2}}. \tag{20}$$

Therefore, with the application of the normalisations in Eq. (19) along with the Gauss-Chebyshev quadrature for N sampling points, equations (8) to (10) yield the following system of non-linear algebraic equations:

$$\frac{\bar{E}}{4N}\sum_{i=1}^{N}\frac{\psi(s_i)}{t_j - s_i} = -\sigma^{\infty} + \sigma_n', \tag{21}$$

$$\frac{\pi a}{N}\sum_{i=1}^{N}\psi(s_i) = 0, \tag{22}$$

$$\delta(t_j) = \frac{\pi a}{N}\sum_{i=1}^{j}\psi(s_i)\,; \tag{23}$$

with $i = 1, 2 \ldots N$, $j = 1, 2 \ldots N-1$ and s_i, t_j being the discrete integration and collocation points of the Gauss-Chebyshev method given, respectively, by

$$s_i = \cos\left(\pi\frac{2i-1}{2N}\right) \tag{25a}$$

and

$$t_j = \cos\left(\pi\frac{j}{N}\right). \tag{25b}$$

The numerical equations detailed above can be solved computationally without serious difficulties by employing standard numerical iterative procedures.

5.2 Computational formulation

The system of equations presented above can be rewritten in matrix form. The main advantage of working with arrays is that its utilisation provides a concise formulation which can be easily implemented computationally. Thus, consider the following set of arrays:

$$\mathbf{W} = \begin{bmatrix} W_{1,1} & W_{1,2} & \cdots & W_{1,N} \\ W_{2,1} & W_{2,2} & \cdots & W_{2,N} \\ \vdots & \vdots & \ddots & \vdots \\ W_{N,1} & W_{N,2} & \cdots & W_{N,N} \end{bmatrix}, \tag{25}$$

$$\boldsymbol{\psi}^T = \{\psi_1 \quad \psi_2 \quad \cdots \quad \psi_N\}, \tag{26}$$

$$\mathbf{S}^T = \{S_1 \quad S_2 \quad \cdots \quad S_N\}. \tag{27}$$

The matrix **W**, which may be termed as the Cauchy kernel matrix, has its elements given by

$$W_{j,i} = \frac{\bar{E}}{4N}\frac{1}{(t_j - s_i)}, \tag{28a}$$

$$W_{N,i} = \frac{a\pi}{N}. \tag{28b}$$

Whereas the components of the stress vector $\mathbf{S}$ are

$$S_j = -\sigma^{\infty} + \sigma'_n, \tag{29a}$$

$$S_N = 0; \tag{29b}$$

with $i = 1, 2 \ldots N$, $j = 1, 2 \ldots N-1$ and with σ'_n given by Eq. (11).

The multiplication of $\mathbf{W}$ and the dislocation vector $\boldsymbol{\psi}$ yields a vector which components are analogous to the left hand side of equations (21) and (22). The right hand side of those equations is given by the components of the stress vector $\mathbf{S}$. Therefore, the elements of the dislocation vector ψ_i, which represent the value of the unknown function ψ at the point s_i $\left(\psi_i = \psi(s_i)\right)$, can be obtained from the solution of the following $N \times N$ system of linear equations:

$$\mathbf{W}\boldsymbol{\psi} = \mathbf{S}. \tag{30}$$

5.3 Stress Analysis

Once an appropriate solution for the unknown function $\psi(s_i)$ is obtained it is then possible to carry out stress analyses.

From an asymptotic analysis the stress intensity factor K can be obtained from the following expression:

$$K = \frac{4}{\bar{E}}\sqrt{\pi a}\psi(\pm 1). \tag{31}$$

Equation (19) gives the residual opening as a function of $\psi(s_i)$ and from equations (5) and (6) the stresses along the fracture opening can be found as

$$\sigma_{xx}(t_j) = \frac{\bar{E}}{4N}\sum_{i=1}^{N}\frac{\psi(s_i)}{t_j - s_i} \tag{32}$$

and

$$\sigma_{yy}(t_j) = \frac{\overline{E}}{4N}\sum_{i=1}^{N}\frac{\psi(s_i)}{t_j - s_i} + \sigma^{\infty}. \tag{33}$$

The out-of-plane stress component $\sigma_{zz}(t_j)$ is found from Eq. (7). Equations (31) – (33) provide the full stress field in the surrounding medium due to the presence of the fracture filled with compressible particles.

6. Physical Remarks

Despite having a different nature, the modelling approach utilised in this paper can be applied to solve many other non-linear problems of Fracture Mechanics. For example, a comparison of the present approach with Cox and Rose (1996) analytical results on the modelling of the non-linear behaviour of composite patching repair of fatigue cracks is presented in the Appendix. This comparison was used to validate the current approach and assess its accuracy. As one can see from the upcoming comparison the highly accurate results can be obtained at relatively high number of integration points. Below, the solutions obtained using the formulation presented earlier are analysed in light of the physical behaviour expected.

6.1 Hydraulic Fracture Residual Opening and Stress Response

From the developed approach derived above (Sections 2 to 5) it is possible to describe both the fracture profiles and the stress response of hydraulic fractures either fully or partially filled with proppants.

The dependences in Fig. 3 provide a succinct view of the fracture residual profile for different cases of proppant placement inside the fracture. In this figure the normalised fracture face displacement, U, was plotted against the normalised position along the fracture, t (see Eq. (19b)). The proppant placement is described by the variation of the ratio b/a, see Fig. 2 for definitions. In the presented calculations the initial porosity, ϕ_0, and the normalised stress, P, where kept at constant values. The normalised values U and P are given, respectively, by

$$U = \frac{\bar{E}}{4a(\sigma^{\infty} + p)}\delta(x) \tag{34}$$

and

$$P = \frac{\bar{E}_s}{\bar{E}}\frac{\sigma_n'(x=0)}{(p+\sigma^{\infty})}. \tag{35}$$

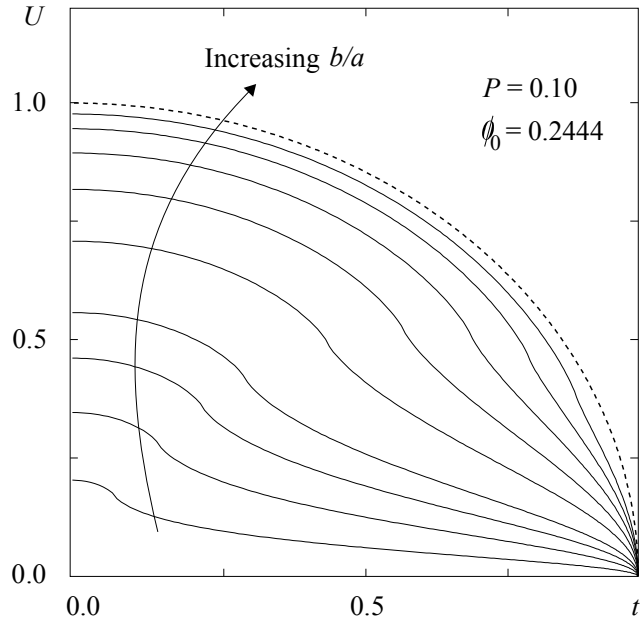

Fig. 3 Fracture normalised residual profiles for a variety of b/a ratios. The dashed curve represents the fracture normalised initial opening. When $b/a = 0$, $U(t) = 0$

From Fig. 3 an abrupt drop in the fracture residual opening profile curve is observed when $t = b/a$ is relatively small due to the lack of the support provided by the proppants inside the fracture. At small values of b/a, the residual opening, as expected, is limiting to zero but this cannot be the case in practice as there are other mechanisms, which can prevent the full closure of the opened fractures. One of such mechanisms is the roughness induced crack opening, which can dominate in the case when the particles were not injected with the pressurised fluid or when the proppants occupy a relatively short portion of the total length of the fracture (Dyskin and Galybin 2001; Kotousov et al. 2011).

The behaviour of the effective stresses acting on the proppant over the crack length is depicted in Fig. 4 for a few different cases of proppant placement. The

latter is once again described by the variation of the ratio b/a whereas the normalised stress over the proppant pack, P', is simply described as

$$P' = \frac{\sigma_n'}{\sigma^\infty}. \tag{36}$$

The initial porosity, ϕ_0, and the normalised stress, P, where also maintained at constant values.

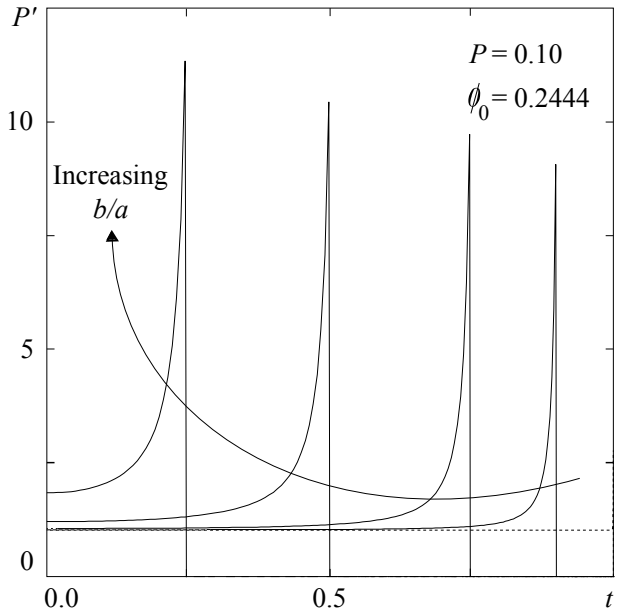

Fig. 4 Proppant pack normalised stress response for different b/a ratios. The dashed curve represents the stress over the proppant pack when the crack is fully filled, i.e. $b/a = 1$. When $t > b/a$, $P'(t) = 0$

It can be realised from Fig. 4 that when the hydraulic fracture is fully filled with proppant, i.e. $b/a = 1$, the proppant pack stress response magnitude matches the one from the confining stress, i.e. $P'(t) = 1$. For situations where $b/a < 1$ the stresses over the proppant pack magnitudes are extremely high at the edge of the proppant pack, i.e. at $t = b/a$, and have a tendency to approach the confining stress magnitude as t closes to zero, i.e. $P'(t \to 0) \to 1$.

The high stresses occurring over the proppant pack when the ratio b/a is sufficiently small is very beneficial as it may help preventing proppant flowback, a phenomenon which restricts well production and that has been the subject of several studies in the past (Nguyen and Jaripatke 2009). Hence, an optimum

balance between the proppant placement and the fracture residual opening must be found in order to maximise well production rate.

6.2 Stress Intensity Factor

It can be noticed from what was discussed above that the crack closure has a strong non-linear behaviour influenced by the proppant distribution and mechanical properties. Nonetheless, the homogeneous elastic-linear medium assumption adopted (Section 2) means that the crack tip behaviour and stress state is dictated by the stress intensity factor – an elastic-linear parameter.

Therefore, the latter provides two limiting cases to assess and validate the residual opening of a fluid driven fracture filled with particles. The first limit corresponds to the situation when the stress intensity factor K is approaching the initial value of the stress intensity factor K_0. This case takes place when the fracture is fully filled $(b/a = 1)$ with hardly compressible particles. The second limiting case manifests that K approaches zero when the fracture opening is fully filled with highly compressive particles or when the placement length of the proppant b is very short. The formulation presented earlier (Sections 2 to 4) fully complies with these limitations.

A normalised stress intensity factor, K_N^*, is introduced as

$$K_N^* = K/K_0. \tag{37}$$

The dependences presented in Fig. 5 clearly demonstrate the tendency of K approaching K_0, i.e. $K_N^* \to 1$, if the fracture is fully filled with relatively stiff particles $(P \geq 0.1)$. This case also corresponds to the maximum residual opening of the crack.

If the compressibility of particles is low (or when non-dimensional parameter P, see Eq. (35), is less then 10^{-4}) then K tends to zero, i.e. $K_N^* \to 0$. Additionally, Fig. 5 also shows the significant effect of the settled proppants length on the residual opening.

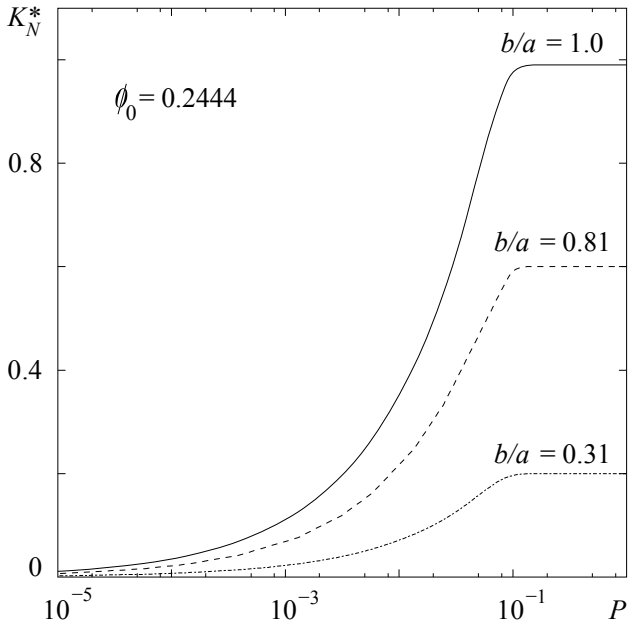

Fig. 5 Normalised stress intensity factor K_N^* versus the normalised stress P for different b/a ratios and constant ϕ_0

7. Conclusions

Despite the residual opening of fractures significantly affecting the permeability of geological reservoirs, and subsequently the well productivity, not much work has been done so far on mechanical and mathematical modelling of this important phenomenon. In this paper we developed a simplified non-linear model of a crack in an infinite linear elastic medium filled with compressible particles and subjected to remote compressive stresses. Further we implemented an effective approach for obtaining numerical results, which is based on the Distributed Dislocation Technique. The approach is very general and can be applied to many other non-linear Fracture Mechanics problems. In particular, it was applied to a completely different problem having a similar mathematical formulation allowing a semi-analytical solution in order to verify the general computational technique. In this work the mechanical response of a pack of low consolidated particles was described by using an earlier developed mathematical model for cohesionless particles. This model provides a reasonable compromise between the accuracy and complexity. However, there are no limitations on the mechanical behaviour or the proppants, which can relatively easy be incorporated into the computational approach.

The underling mechanical model incorporates a number of simplifications needed for the development of the mathematical model. Many of these simplifications, such as 2D fracture geometry and linear elastic behaviour of the surrounding medium, represent a well-established foundation for modelling of hydraulic stimulation techniques. We have not focused on a critical analysis of these assumptions but rather tried to eliminate and evaluate some of them. The current study concentrated on the effect of the particle compressibility ant its distribution along the fracture length on the residual fracture profile. The numerical results obtained within the developed mathematical model indicate that the compressibility and distribution of the proppant inside the fracture have a strong influence of the residual fracture profile and can not be disregarded when assessing the outcomes of the hydraulic stimulations.

Appendix: Validation of the Computational Approach

Cox and Rose (1996) work focused on the modelling of the non-linear behaviour of composite patching repair of fatigue cracks when a notch of length b is present. Despite having a different nature, its mathematical formulation is very similar to the problem considered above. The analytical results presented by these authors were, therefore, adopted as the benchmark for validating the mathematical model described in Section 3. Their solution utilises elastic/perfectly-plastic springs to model the crack bridging patch. Therefore, changes in the formulation presented earlier are needed in order to make the comparisons. The required changes specifically concern the boundary conditions and $\sigma_n'(x)$, being given by:

$$\sigma_{yy}(x,y) = \sigma^{\infty} - \sigma_n'(x), b \le |x| \le a, y = 0; \quad \text{(A.1a)}$$

$$\sigma_n'(x) = \bar{E}k\delta(x), \delta(x) < \delta_p; \quad \text{(A.1b)}$$

$$\sigma_n'(x) = \sigma_p = \bar{E}k\delta_p, \delta(x) \ge \delta_p; \quad \text{(A.1c)}$$

where k is a constant characterising the spring stiffness in the linear range, σ_p is the yield stress, and δ_p is a characteristic crack opening beyond which the spring response changes from being elastic to being perfectly plastic, see Cox and Rose,

1996. Additionally, the initial stress intensity factor K_0 and the initial crack opening δ_0 set at zero.

The formulae presented by Cox and Rose (1996) for predicting the stress intensity factor K and the crack opening $\delta(x)$ are, respectively, as follow:

$$K = \sigma^{\infty}\sqrt{\pi a} - 2\sqrt{\frac{a}{\pi}}\int_{b}^{a}\frac{\sigma_n'(x)}{\sqrt{a^2 - x^2}}\mathrm{d}x, \tag{A.2}$$

$$\delta(x) = 4\frac{\sigma^{\infty}}{\bar{E}}\sqrt{a^2 - x^2} - \frac{4}{\pi\bar{E}}\int_{b}^{a}\ln\left|\frac{\sqrt{a^2 - \xi^2} + \sqrt{a^2 - x^2}}{\sqrt{a^2 - \xi^2} - \sqrt{a^2 - x^2}}\right|\sigma_n'(\xi)\mathrm{d}\xi. \tag{A.3}$$

These formulae can be rewritten in a numerical fashion and solved numerically.

A concise description of the employed algebraic manipulations and obtained results can be achieved by the adoption of the following normalisations:

$$A = \frac{4ka}{\pi}, \tag{A.4a}$$

$$B = \frac{4kb}{\pi}, \tag{A.4b}$$

$$K_N = \frac{K\sqrt{k}}{\sigma_p}. \tag{A.4c}$$

A being the normalised crack length, B the normalised notch length and K_N the normalised stress intensity factor.

The development of the normalised stress intensity factor K_N for various normalised fracture lengths A as predicted by the above developed formulation, for a varying N, is compared against Cox and Rose (1996) approach (equations (A.2) and (A.3)). Such comparison is presented in Fig. A.1, which provides a succinct overview of the solutions obtained.

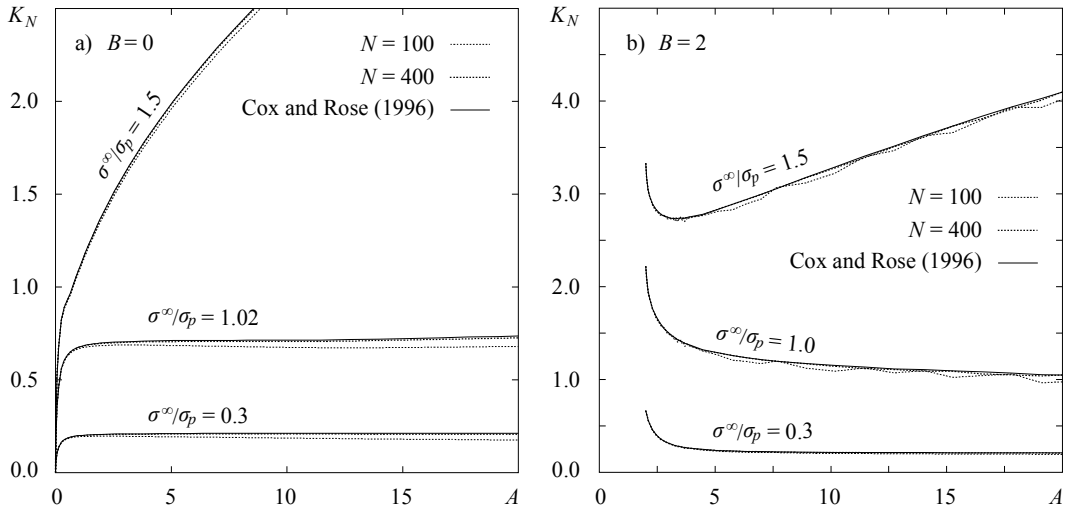

Fig. A.1 Normalised stress intensity factor K_N development for both elastic and elastic/perfectly-plastic cases. Situations (a) with zero notch length $(B = 0)$ and (b) with moderate notch length $(B = 2)$ are shown

The comparison presented in Fig. A.1 demonstrates a good agreement between the numerical approach derived above and the results presented by Cox and Rose (1996). The difference totally disappears with an increase of the number of integration points in the numerical solution.

Acknowledgments

The authors gratefully acknowledge the support provided by the Australian Research Council via research grants DP1094299 and LP100100613.

References

Adachi J, Siebritsb E, Peircec A, Desroches J (2007). Computer simulation of hydraulic fractures. *Int J Rock Mechanics and Mining Sciences*, 44(5), pp.739–757.

Barenblatt GI, Entov VM, Ryzhik V (1990). *Theory of Fluid Flows Through Natural Rocks* 1st ed., Springer.

Bilby B, Eshelby J (1968). Chapter 2: Dislocations and the theory of fracture. In *Fracture: An Advanced Treatise*. New York: Academic Press, pp. 99–182.

Bortolan Neto L, Kotousov A, Bedrikovetsky P (2011a). Application of Contact Theory to Evaluation of Elastic Properties of Low Consolidated Porous Media. *Int J Fracture*, 168(2), pp.267–276.

Bortolan Neto L, Kotousov A, Bedrikovetsky P (2011b). Elastic properties of porous media in the vicinity of the percolation limit. *J Petroleum Science and Engineering*, 78(2), pp.328–333.

Clark PE, Güler N (1983). Prop Transport in Vertical Fractures: Settling Velocity Correlations. In SPE/DOE Low Permeability Gas Reservoirs Symposium. Denver, Colorado: SPE 11636-MS, p. 6.

Clifton RJ, Wang J-J (1988). Multiple Fluids, Proppant Transport, and Thermal Effects in Three-Dimensional Simulation of Hydraulic Fracturing. In SPE Annual Technical Conference and Exhibition. Houston, Texas: SPE 18198-MS, p. 14.

Cox BN, Rose LRF (1996). A self-consistent approximation for crack bridging by elastic/perfectly plastic ligaments. *Mechanics of Materials*, 22(4), pp.249–263.

Cutler RA, Enniss DO, Jones AH, Swanson SR (1985). Fracture Conductivity Comparison of Ceramic Proppants. *Society of Petroleum Engineers Journal*, 25(2), pp.157–170.

Dam DB, Pater CJ, Romijn R (2000). Analysis of Hydraulic Fracture Closure in Laboratory Experiments. *SPE Production & Facilities*, 15(3).

Daneshy AA (1975). Numerical Solution of Sand Transport in Hydraulic Fracturing. In SPE 50th Annual Fall Meeting. Dallas, Texas: SPE 5636.

Daneshy AA (1978). Numerical Solution of Sand Transport in Hydraulic Fracturing. *J Petroleum Technology*, 30(1), pp.132–140.

Dyskin AV, Galybin AN (2001). Solutions for dilating shear cracks in elastic plane. *Int J Fracture*, 109(3), pp.325–344.

Economides MJ, Nolte KG (2000). *Reservoir Stimulation* 3rd ed., Chichester: Wiley.

Entov VM, Murzenko VV (1994). Steady flow of homogeneous fluid in an oil reservoir recovery element with a hydrofracture. *Fluid Dynamics*, 29(1), pp.81–87.

Gadde PB, Liu Y, Norman J, Bonnecaze R, Sharma MM (2004). Modeling Proppant Settling in Water-Fracs. In SPE Annual Technical Conference and Exhibition. Houston, Texas: SPE 89875-MS, p. 10.

Golf-Racht TD van (1982). *Fundamentals of Fractured Reservoir Engineering*, Elsevier.

Hertz H (1896). *Miscellaneous papers* D. E. Jones & G. A. Schott, eds., New York: MacMillan.

Hills DA, Kelly PA, Dai DN, Korsunsky AM (1996). *Solution of crack problems: the distributed dislocation technique*, London: Kluwer Academic Publishers.

Johnson KL (1985). *Contact Mechanics*, Cambridge [Cambridgeshire]: Cambridge University Press.

Johnson KL (1982). One hundred years of hertz contact. *ARCHIVE: Proceedings of the Institution of Mechanical Engineers 1847-1982 (vols 1-196)*, 196(1982), pp.363–378.

Kanevskaya RD, Kats RM (1996). Exact solutions of problems of fluid inflow into a well with a vertical hydrofracture and their use in numerical models of flow through porous media. *Fluid Dynamics*, 31(6), pp.854–864.

Kern LR, Perkins TK, Wyant RE (1959). The Mechanics of Sand Movement in Fracturing. *J Petroleum Technology*, 11(7), pp.55–57.

Kotousov A, Bortolan Neto L, Rahman SS (2011). Theoretical model for roughness induced opening of cracks subjected to compression and shear loading. *Int J Fracture*, 172(1), pp.9–18.

Kotousov A, Codrington JD (2010). Chapter 5: Application of Refined Plate Theory to Fracture and Fatigue. In S. Y. Ho, ed. *Structural Failure Analysis and Prediction Methods for Aerospace Vehicles and Structures*. Sharjah, UAE: Bentham Science Publishers, pp. 90–103.

Mahrer KD (1999). A review and perspective on far-field hydraulic fracture geometry studies. *J Petroleum Science and Engineering*, 24(1), pp.13–28.

Montgomery CT, Steanson RE (1985). Proppant Selection: The Key to Successful Fracture Stimulation. *J Petroleum Technology*, 37(12).

Murzenko VV (1994). Exact solutions of problems of steady fluid flow in reservoirs with hydrofractures. *Fluid Dynamics*, 29(2), pp.214–220.

Nguyen P, Jaripatke O (2009). Controlling Solids Flowback to Maintain Production of Hydrocarbons: A Review of Successful Chemical Technologies in the Last Decade. In International Petroleum Technology Conference. Doha, Qatar: SPE 13725-MS, p. 18.

Novotny EJ (1977). Proppant Transport. In SPE Annual Fall Technical Conference and Exhibition. Denver, Colorado: SPE 6813-MS, p. 12.

Panayiotopoulos KP (1989). Packing of sands - A review. *Soil and Tillage Research*, 13(2), pp.101–121.

Papanastasiou P (2000). Hydraulic fracture closure in a pressure-sensitive elastoplastic medium. *Int J Fracture*, 103(2), pp.149–161.

Pyrak-Nolte LJ, Myer LR, Cook NGW, Witherspoon PA (1987). Hydraulic and Mechanical Properties of Natural Fractures In Low Permeability Rock. In *6th ISRM Congress*. Montreal, Canada: Int Society for Rock Mechanics, p. 7.

Rahman MM, Rahman MK (2010). A Review of Hydraulic Fracture Models and Development of an Improved Pseudo-3D Model for Stimulating Tight Oil/Gas Sand. *Energy Sources, Part A: Recovery, Utilization, and Environmental Effects*, 32(15), pp.1416–1436.

Secchi S, Schrefler BA (2012). A method for 3-D hydraulic fracturing simulation. *Int J Fracture*, 178, pp.245-258.

Smith MB, Klein HH (1995). Practical Applications of Coupling Fully Numerical 2-D Transport Calculation with a PC-Based Fracture Geometry Simulator. In SPE Annual Technical Conference and Exhibition. Dallas, Texas: SPE 30505.

Unwin AT, Hammond PS (1995). Computer Simulations of Proppant Transport in a Hydraulic Fracture. In SPE Western Regional Meeting. Bakersfield, California: SPE 29649-MS, p. 16.

Vincent MC (2002). Proving It - A Review of 80 Published Field Studies Demonstrating the Importance of Increased Fracture Conductivity. In SPE Annual Technical Conference and Exhibition. San Antonio, Texas: Society of Petroleum Engineers, p. 21.

Wahl H, Campbell J (1963). Sand Movement in Horizontal Fractures. *J Petroleum Technology*, 15(11), pp.1239–1246.

Walsh JB (1981). Effect of pore pressure and confining pressure on fracture permeability. *Int J Rock Mechanics and Mining Sciences & Geomechanics Abstracts*, 18(5), pp.429–435.

Warpinski NR, Moschovidis ZA, Parker CD, Abou-Sayed IS (1994). Comparison Study of Hydraulic Fracturing Models—Test Case: GRI Staged Field Experiment No. 3. *SPE Production & Facilities*, 9(1), pp.7–16.

Zazovskii AF, Todua GT (1991). Steady inflow into a well with a long vertical fracture. *Fluid Dynamics*, 25(4), pp.584–593.